

Influence of Heat Exchanger Tube Configuration on Simultaneous Charging and Discharging Performance of LHTES[#]

Ikhtedar Husain Rizvi¹, Dibakar Rakshit^{1*}, B. Premachandran², K. Ravi Kumar¹, K. S. Reddy³

¹Department of Energy Science and Engineering, IIT Delhi, New Delhi-110016, India

² Department of Mechanical Engineering, IIT Delhi, New Delhi-110016, India

³ Department of Mechanical Engineering, IIT Madras, Chennai-600036, India

(Corresponding Author: Dibakar.Rakshit@iitd.ac.in)

ABSTRACT

This study investigates the effect of heat transfer tube configurations on the thermal performance of latent heat thermal energy storage systems operating under simultaneous charging and discharging conditions. A two-dimensional numerical model was developed using the enthalpy–porosity method to simulate melting and solidification of phase change material. Four tube arrangements, comprising two charging and two discharging tubes, were analyzed to evaluate their impact on melting/solidification progression and heat flux variation. Results indicate that tube placement significantly influences natural convection within the PCM, thereby affecting energy transfer rates. Case 4 shows the highest initial charging heat flux due to enhanced early convection, but Case 2 sustains the highest long-term fluxes during both charging (1000 W/m²) and discharging (900 W/m²). Case 3 consistently demonstrates poor performance, highlighting unfavorable flow pathways. Overall, Case 2 emerges as the most effective configuration, offering an optimal balance between charging and discharging performance. These findings highlight the importance of tube geometry in designing high-efficiency LHTES units for continuous energy supply applications.

Keywords: Latent Heat Thermal Energy Storage, Simultaneous Charging and Discharging, Heat Transfer Tube Configuration, Phase Change Materials, Thermal Performance.

NONMENCLATURE

Abbreviations

LHTES	Latent Heat Thermal Energy Storage
SCD	Simultaneous Charging and Discharging
HTF	Heat Transfer Fluid

PCM	Phase Change Material
<i>Symbols</i>	
ρ	Density (kg/m ³)
t	Time (s)
\vec{v}	Velocity Vector (m/s)
p	Pressure (Pa)
\vec{g}	Gravity coefficient (m/s ²)
β	Thermal expansion coefficient (K ⁻¹)
λ	Liquid fraction (-)
T	Temperature (K)
H	Enthalpy (J)
L	Latent heat (J)
c_p	Specific heat capacity (J)
k	Thermal conductivity (w/m-K)

1. INTRODUCTION

Thermal energy harnessed from renewable sources is inherently intermittent and not always available when needed. Therefore, effective energy storage becomes essential. Phase Change Materials (PCMs) are a promising option due to their high capacity for storing large amounts of thermal energy within a narrow temperature range. Moreover, PCMs offer wide applicability [1-3], as materials are available with melting points spanning from low to high temperatures, making them suitable for diverse applications.

Latent heat thermal energy storage (LHTES) systems are widely used to store and release thermal energy efficiently [3-6]. The performance of these systems significantly depends on the thermal conductivity of the phase change material (PCM) and the configuration of the heat transfer tubes. The utilisation of fins has been shown to enhance LHTES performance. Tree-shaped fin

[#] This is a paper for the 17th International Conference on Applied Energy (ICAE2025), December 8-12, 2025, Bangkok, Thailand.

structures in triplex tube heat exchangers reduced melting/solidification times by up to 7.36% and 23.70%, also minimizing unmelted PCM regions for more uniform phase transition [7]. The application of wavy channel geometries in triplex-tube LHTES units significantly enhances PCM solidification. Step-function channels reduced discharge time by over 65% and boosted heat recovery by nearly 148% compared to straight channels [8]. Using the multiple heat transfer tubes in LHTES systems enhances convective heat transfer and minimises orientation effects, reducing melting time differences from 30 min to 3.5 min in comparison to a single tube configuration. Despite higher pumping power, faster charging makes multi-tube designs more efficient [9,10]. In recent years, simultaneous charging and discharging (SCD) operations have gained attention for their ability to provide a continuous thermal energy supply [11,12]. However, SCD introduces complex thermal interactions within the storage unit, making it essential to optimize the heat transfer tube configuration for effective thermal management [13,14].

This study focuses on investigating the influence of the tube arrangements on the total melting time, melting/solidification front movement, and overall performance during SCD operations.

2. MATERIALS AND METHODS

A two-dimensional numerical model was developed using the enthalpy-porosity [15] technique to simulate the melting and solidification of PCM under SCD conditions. The governing equations for mass, momentum, and energy conservation were solved using the finite volume method. The PCM material is considered isotropic and homogenous with no volume change during the phase change process, and the natural convection is modelled by the Boussinesq approximation. Viscous dissipation is neglected during phase change, considering natural convection movement of the PCM. Fig. 1 shows the validation of the adapted methodology with experimental results of Siyabi et al. [16].

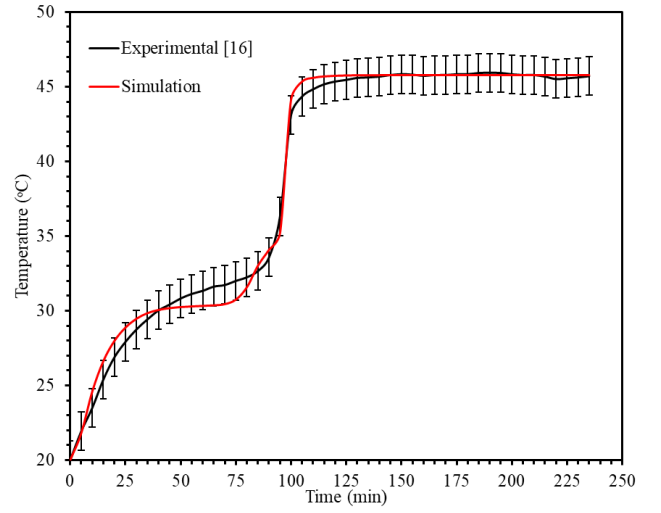


Fig.1 Validation of current model.

$$\frac{\partial \rho}{\partial t} + \nabla \cdot (\rho \vec{V}) = 0 \quad (1)$$

$$\frac{\partial \rho \vec{V}}{\partial t} + \nabla \cdot (\rho \vec{V} \vec{V}) = -\nabla p + \nabla \cdot (\mu \nabla \vec{V}) + \vec{g} \beta \rho_{ref} (T - T_{ref}) + S \quad (2)$$

$$S = \frac{(1-\lambda)^2}{\lambda^3 + \epsilon} A_{mushy} \vec{V} \quad (3)$$

$$\lambda = \begin{cases} 0, & \text{if } T \leq T_{solidus} \\ \frac{T - T_{solidus}}{T_{liquidus} - T_{solidus}}, & \text{if } T_{solidus} < T < T_{liquidus} \\ 1, & \text{if } T \geq T_{liquidus} \end{cases} \quad (4)$$

$$\frac{\partial (\rho H)}{\partial t} + \nabla \cdot (\rho \vec{V} H) = \nabla \cdot (k \nabla T) \quad (5)$$

$$H = h_{ref} + \int_{T_{ref}}^T m c_p dT + \lambda L \quad (6)$$

Table 1: Material Properties

Parameter	PCM
Density (kg/m ³)	720
Specific heat (J/kg-K)	2000
Thermal conductivity (w/m-K)	0.25
Dynamic viscosity (Pa-s)	0.025
Thermal expansion coefficient (1/K)	0.0001
Latent heat (J/kg)	160000
Solidus temperature (K)	307
Liquidus temperature (K)	309

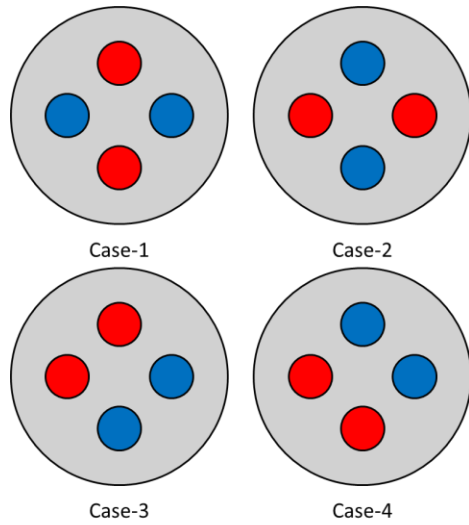


Fig. 2 Schematic of the cases considered.

The constant temperature boundary conditions were defined to simulate SCD at different locations of the storage system. Charging tubes are set at a temperature of 328 K, and discharging tubes are set at a temperature of 288 K, which is sufficient above and below the melting point of PCM. The initial condition of the PCM material was set at 298 K, considering the normal ambient condition. The four cases considered for the analysis are shown in Fig. 2.

3. RESULTS AND DISCUSSION

Fig. 3 presents the average liquid fraction of the storage domain, starting from an initial temperature of 25°C. Initially, the melt fraction progresses similarly across all cases. However, as natural convection becomes dominant, the liquid fraction increases more rapidly in Case 4 and more slowly in Case 3. In Case 4, the tube configuration promotes effective convection by covering the bottom and mid-sections, allowing the heated PCM to rise and facilitating greater circulation of the liquid PCM. This results in enhanced heat transfer and a faster melting rate.

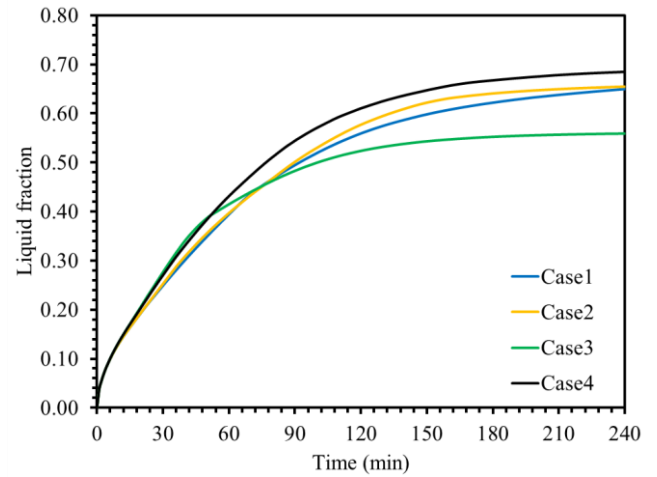


Fig. 3 Average Liquid fraction of the PCM domain.

Fig. 4 illustrates the liquid fraction contours for the tube configurations considered at four different time instants: 1800 s, 3600 s, 5400 s, and 7200 s. The colour scale indicates the liquid fraction, with blue representing the solid phase and red indicating the fully melted region. Before 1800 s, melting is primarily dominated by conduction, and the liquid fraction remains low across all cases. The regions adjacent to the heat transfer tubes begin to melt first, forming thin liquid layers around the tubes. Minimal differences between the cases are observed at this early stage. By 3600 s, the effect of natural convection becomes more prominent. In Case 4, the melting front advances rapidly from the bottom and mid-section of the domain, taking advantage of the vertical movement of the heated liquid PCM. This results in a significantly larger liquid fraction compared to other cases. In contrast, Case 3 shows slower melting progression, as the tube arrangement limits the effective flow paths for convection, restricting heat transfer to the upper regions. At 5400 s, the disparities in melting progression between configurations become more evident. Case 4 continues to exhibit accelerated melting, covering a larger portion of the domain with liquid PCM. Cases 1 and 2 show moderate melting rates, while Case 3 still demonstrates the slowest melting progression due to unfavourable convection currents and limited heat transfer surface area. By the final time instant of 7200 s, Case 4 achieves the highest melting, indicating high storage capability under simultaneous charging and discharging conditions. The other cases show less melting, with significant solid PCM still present, especially in Case 3. This highlights the critical role of heat transfer tube placement in enhancing natural convection effects and accelerating the melting process.

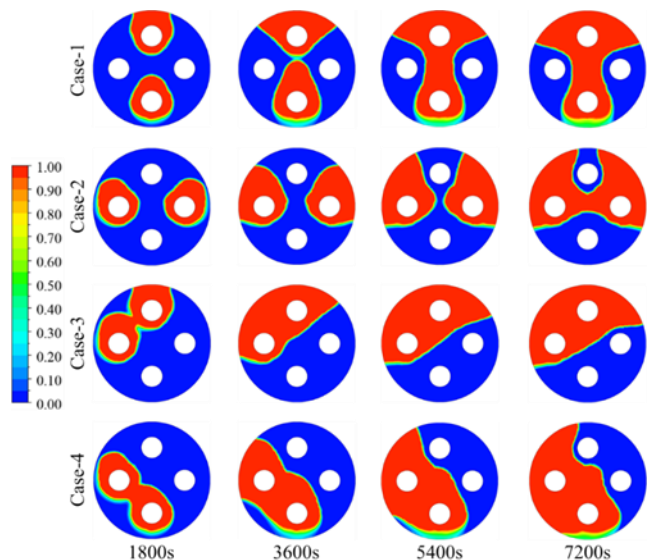


Fig. 4 Contours of liquid fraction propagation.

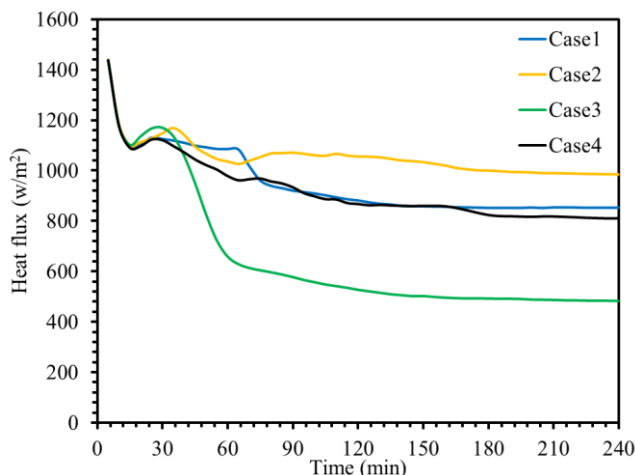


Fig. 5 Variation of charging heat flux for considered cases.

Fig. 5 and 6 present the charging and discharging heat flux variations under SCD conditions for the four heat transfer tube configurations. The charging rate, all cases initially show a sharp rise in heat flux due to the large temperature difference between the HTF and the PCM. Case 4 exhibits the highest initial peak (~ 1450 W/m^2), indicating its strong ability to accelerate the early melting process. However, as the process continues, the charging heat flux of Case 4 gradually declines and stabilizes around ~ 800 W/m^2 . Case 2, on the other hand, demonstrates superior long-term performance, sustaining the highest steady flux (~ 1000 W/m^2) throughout the operation. Case 1 maintains moderate performance (~ 850 W/m^2), while Case 3 shows the weakest charging capability, dropping below 600 W/m^2 after 60 minutes due to limited convective heat transfer paths.

For the discharging rate (Fig. 6), a similar trend is observed. After an initial decline, Case 2 recovers strongly, with its heat flux increasing steadily to about 900 W/m^2 , ensuring effective energy release over an extended duration. Cases 1 and 4 show moderate recovery, stabilizing around 800 W/m^2 , while Case 3 again remains the least effective, falling below 500 W/m^2 . These results indicate that tube placement plays a critical role in governing natural convection effects and optimizing heat transfer. Overall, Case 2 consistently outperforms the other configurations in SCD, making it the most effective design for stable and efficient SCD operation in latent heat thermal energy storage systems.

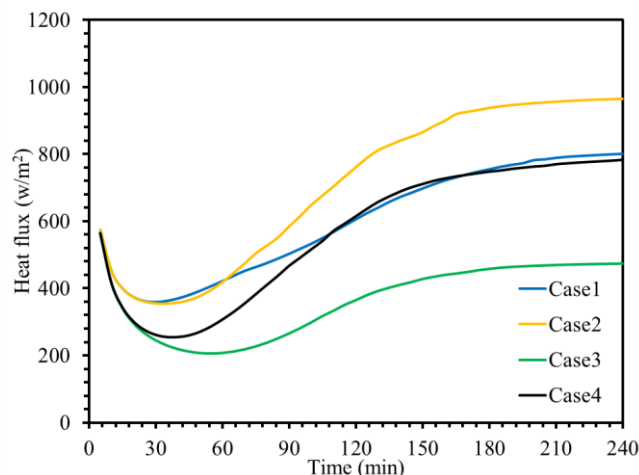


Fig. 6 Variation of discharging heat flux for considered cases.

4. CONCLUSIONS

This study numerically examined the influence of heat transfer tube configurations on the performance of LHTES systems under SCD conditions. Four different tube arrangements were analyzed to evaluate their effects on melting and solidification behavior and heat flux variation.

The results demonstrate that tube placement strongly governs the natural convection patterns within the PCM, thereby affecting both charging and discharging rate. Case 4 exhibited the highest initial charging heat flux due to favorable tube positioning, but its performance gradually declined with time. Case 2, in contrast, sustained the highest long-term heat fluxes during both charging (1000 W/m^2) and discharging (900 W/m^2), confirming its optimal charging and discharging. Case 1 offered moderate and stable performance, while Case 3 consistently showed the lowest flux values, highlighting ineffective convection pathways and reduced thermal interaction.

Overall, Case 2 is identified as the most effective configuration, providing an optimal balance between rapid charging and sustained discharging performance. These findings emphasize the critical role of tube configuration in enhancing thermal management of LHTES systems and can guide the design of more efficient storage units for continuous energy supply applications.

ACKNOWLEDGEMENT

The financial support for this research work is provided by the Department of Science and Technology (DST), Government of India, New Delhi, through the research project (Project Number: DST/TMD/CERI/RES/2020/14(G)).

REFERENCE

- [1] Rizvi IH. A modified Kalman filter-based model for core temperature estimation during exercise and recovery with/without personal cooling interventions. *Journal of Thermal Biology*. 2022;109:103307.
- [2] Jain S, Rizvi IH, Kumar KR, Rakshit D, Premachandran B, Reddy KS. Versatile cascade latent heat storage system for smoke-free indoor solar cooking. *Solar Energy*. 2025;300:113872.
- [3] Gupta SK, Rizvi IH, Premachandran B, Rakshit D, Kumar KR, Reddy KS. Field study of sustainable space heating systems coupled with thermal energy storage for thermal comfort. *Energy and Buildings*. 2025;352:116850.
- [4] Mahdi JM, Lohrasbi S, Ganji DD, Nsofor EC. Simultaneous energy storage and recovery in the triplex-tube heat exchanger with PCM, copper fins and Al₂O₃ nanoparticles. *Energy conversion and management*. 2019;180:949-61.
- [5] Joybari MM, Haghighat F, Seddegh S, Al-Abidi AA. Heat transfer enhancement of phase change materials by fins under simultaneous charging and discharging. *Energy Conversion and Management*. 2017;152:136-56.
- [6] Joybari MM, Haghighat F, Seddegh S. Numerical investigation of a triplex tube heat exchanger with phase change material: Simultaneous charging and discharging. *Energy and buildings*. 2017;139:426-38.
- [7] Esmaeili Z, Vahidhosseini SM, Rashidi S. Enhancing latent heat thermal energy storage in triplex tube heat exchangers using tree-shaped fin structures with novel branching methods. *Journal of Energy Storage*. 2024;97:112970.
- [8] Said MA, Togun H, Abed AM, Biswas N, Mohammed HI, Sultan HS, Mahdi JM, Talebizadehsardari P.

Evaluation of wavy wall configurations for accelerated heat recovery in triplex-tube energy storage units for building heating applications. *Journal of Building Engineering*. 2024 Oct 1;94:109762.

- [9] Rizvi IH, Rakshit D, Premachandran B, Kumar KR, Reddy KS. Impact of multi-tube configurations on pumping power and heat transfer rate at different orientations of latent heat thermal energy storage systems. *Journal of Energy Storage*. 2025;114:115753.
- [10] Kishor V, Kumar R, Singh S, Srivastava A. Nonintrusive experimental study of natural convection in an open square cavity at different inclinations. *Journal of Flow Visualization and Image Processing*. 2020;27(3).
- [11] Joybari MM, Haghighat F, Seddegh S, Yuan Y. Simultaneous charging and discharging of phase change materials: Development of correlation for liquid fraction. *Solar Energy*. 2019;188:788-98.
- [12] Liu Z, Wang Z, Ma C. An experimental study on the heat transfer characteristics of a heat pipe heat exchanger with latent heat storage. Part II: Simultaneous charging/discharging modes. *Energy conversion and management*. 2006;47(7-8):967-91.
- [13] Sharifi, N., Faghri, A., Bergman, T. L., & Andracka, C. E. (2015). Simulation of heat pipe-assisted latent heat thermal energy storage with simultaneous charging and discharging. *International Journal of Heat and Mass Transfer*, 80, 170-179.
- [14] Wang, Z., Diao, Y., Zhao, Y., Chen, C., Liang, L., & Wang, T. (2019). Thermal performance investigation of an integrated collector-storage solar air heater based on lap joint-type flat micro-heat pipe arrays: Simultaneous charging and discharging mode. *Energy*, 181, 882-896.
- [15] Voller VR, Prakash C. A fixed grid numerical modelling methodology for convection-diffusion mushy region phase-change problems. *International journal of heat and mass transfer*. 1987;30(8):1709-19.
- [16] Al Siyabi I, Khanna S, Mallick T, Sundaram S. An experimental and numerical study on the effect of inclination angle of phase change materials thermal energy storage system. *Journal of Energy Storage*. 2019;23:57-68.